Indian Journal of Chemical Technology
Vol. 23, November, 2016 pp. 462-468

A green and facile synthesis of silver nanoparticles and its application in the reduction and photodegradation of organic compounds

Tanur Sinha, M Ahmaruzzaman* & Archita Bhattacharjee

Department of Chemistry, National Institute of Technology, Silchar 788 010, India
E-mail: md_2002@rediffmail.com

Received 26 September 2014; accepted 5 November 2015

A simple, environment friendly, and microwave assisted green synthesis of silver nanoparticles (Ag NPs) depicting the dual functional properties of lithium dodecyl sulphate as a co-reducing and stabilizing agent has been presented. This is a rapid (6 min) and economic protocol that avoids the use of additional external capping agents, external reducing agents, solvents and templates. The method results in rapid formation of spherical Ag NPs with average sizes in the range of ~7-15 nm. The possible mechanism for the formation of Ag NPs has also been presented. The synthesised Ag NPs have been characterised by various techniques, such as UV vis spectroscopy, Transmission electron spectroscopy and X-RD analysis. The prepared Ag NPs exhibit good catalytic activities towards the reduction of 4-nitro phenol in aqueous as well as in micellar media and show excellent photocatalytic activities for the removal of methyl violet 6B dye from aqueous phase. Approximately, 98.3% of methyl violet 6B dye is degradation with synthesized Ag NPs during the photocatalytic degradation process.

Keywords: Lithium dodecyl sulphate, Methyl violet 6B dye, *Para*-nitrophenol photodegradation, Reduction, Silver nanoparticles

The noble nanometals, especially silver nanoparticles (Ag NPs) have received immense attractions owing to their unique properties, such as surface plasmon resonance (SPR) giving absorption in the UV- visible spectra arising from the collective oscillations of conducting electrons in metals with electromagnetic radiations[1] and potential applications in various emerging fields, like catalysis, nanoelectronics, biomedicine, sensing and surface-enhanced Raman scattering (SERS)[2]. Various methods are available in the literature for their synthesis[3-5]. However, in all these methods, toxic solvents, aggressive and harmful reducing and stabilising agents are utilized, which are dangerous either from the viewpoint of environment or biological aspects.

Hence, incorporations of green chemistry ideologies which include environmentally benign starting materials, solvent medium, reducing and stabilizing agents into nanoscience and nanotechnologies are very much essential[6]. Investigations have shown that microwave irradiation is considered to be green, more environments friendly, efficient, faster, stable and cleaner than the conventional heating methods. Moreover, microwave heating technique increases the rate of formation, particles size and quality. It also shows yield enhancement, acceleration in reaction rate, small reaction time, highly pure materials, narrow particle size distribution and improved physicochemical properties[7]. So, there is a growing need to utilize microwave irradiation technique for the synthesis of nanoparticles due to its innumerable advantages over the conventional heating method. A simple, faster, cheap, environment friendly and non-toxic microwave assisted one pot synthesis of Ag NPs has been described herein, exploiting the dual functional properties of lithium dodecyl sulphate (LDS) as a stabilizing and co-reducing agent, and eliminating the use of hazardous chemicals and harsh distinct reducing agents like sodium borohydride, hydrazine etc. The synthesised Ag NPs were utilized for the catalytic reduction of 4-nitro phenol (4-NP) in aqueous as well as in micellar media and for the photocatalytic degradation of the methyl violet 6B dye (MV6B) under solar irradiation. Methyl violet 6B was chosen as it is a potential carcinogen, mutagen and miotic poison, and therefore, concerns exist regarding the ecological impact of the release of methyl violet 6B into the environment and photodegradation is one of the important method for

the removal of methyl violet 6B from the environment. The possible mechanism for the formation of Ag NPs has also been discussed.

Experimental Section

Materials

Silver nitrate, Lithium dodecyl sulphate (LDS), sodium borohydride ($NaBH_4$), *p*-nitro phenol (4-NP), sodium dodecyl sulphate (SDS), cetyl pyridinium chloride (CPC), and triton X-100 (TX-100), methyl violet 6B dye (MV6B) of A.R Grade was purchased from Sigma-Aldrich and used as received. Double distilled water was used in all experiments. All the reactions were carried out in a domestic microwave oven of 300 W.

Synthesis of Ag NPs

An aqueous solution of silver nitrate (0.1 M, 10 mL) was taken in a container and of LDS (60 mM 10 mL) was added to it and the mixture was then kept in a microwave oven and irradiated at 70°C at thirty six 10s 300 W shots followed by slow cooling at room temperature. The solution was then allowed to stabilize for 2 h. After 2 h, the solutions with brown sediments were formed at the bottom of the container indicated the presence of Ag NPs. These were then centrifuged, filtered and the residues were washed several times with double distilled water to remove the free dodecylsulphate anions from the synthesised Ag NPs.

Characterization of Ag NPs

The UV-vis absorption spectra of the synthesised Ag NPs were recorded on Cary 100 Bio spectrophotometer (λ_{max} in nm) equipped with 1 cm quartz cell. The Transmission electron microscopy (TEM) and selected area electron diffraction pattern (SAED) were recorded using Jeol-JEM 2100 transmission electron microscope operated at an accelerating voltage of 200 kV. The X ray diffraction (XRD) pattern was recorded by X' Pert Pro X-ray diffractometer (PANalytic B.V.) by using Cu-Kα radiation operating at a voltage of 40 kV and a current of 30 mA.

Catalytic activity of the synthesised silver nanoparticles

In a standard quartz cuvette, having 1 cm path length , 2 mL of water , 60 µL of (6.07×10^{-3} M) 4-nitro phenol and 350 µL of aqueous $NaBH_4$ (0.1 M) was added and the absorbance was noted with a UV-Vis spectrometer. Thereafter, 150 µL of 10% Ag NPs solution was added to that mixture and the absorbance was recorded up to 20 min. The peak due to the 4-NP was no longer observed and a new peak due to SPR of Ag NPs was appeared at ~420 nm.

Photo catalytic activity of the synthesised silver nanoparticles

The photocatalytic activity of the synthesised Ag NPs was evaluated by the degradation of methyl violet 6B (MV6B) under direct sunlight. In order to evaluate the photocatalytic activity, 10 mg of Ag NPs photocatalyst was dispersed by sonication in 200 mL of 10^{-4} M aqueous solution of MV6B. The dye was then exposed to sunlight irradiation. The experiments were carried out on a sunny day at Silchar city between 10 a.m-3 p.m (outside temperature 35-40°C). At a regular interval of time, 4 mL of the suspension was withdrawn and centrifuged immediately to remove Ag NPs. The filtrates were analyzed by recording the variation of the absorption–band maximum of Methyl violet 6B dye in the UV-vis spectrum. The controlled experiment containing only dye solution was also carried out in presence of solar irradiation.

According to Beer- Lambert Law[8,9] , concentration (c) is related to absorbance (A) of a solution by the following equation,

$$A = \varepsilon bc \quad \text{... (1)}$$

where ε is the molar absorption coefficient and b is the thickness of the absorption cell. In this experiment, since all the testing parameters were kept constant, so a and b can be considered as a constant. Therefore, the changes of the concentration of methyl violet solution can be determined using UV-vis spectrophotometer. Since, the concentration of methyl violet was very low, so its photo degradation follows pseudo-first order reaction and its kinetics is given by[10].

$$\ln (C_0/C_t) = K_t \quad \text{... (2)}$$

where K=rate constant, C_0=initial concentration of methyl violet and C_t = concentration of methyl violet dye after degradation.

The percentage efficiency was determined using the following equation[11].

$$X = (C_0\text{-}C) \times 100/C_0 \quad \text{... (3)}$$

where C_0 and C are absorbance, before and after degradation.

Results and Discussion

UV visible, TEM, SAED and XRD analysis

The formation of Ag NPs was confirmed by UV-visible spectral analysis. The progress of the reaction between the silver ions and LDS was monitored by UV-visible spectra of the Ag NPs in aqueous solution (Fig. 1). It is apparent that the peak due to the SPR of Ag NPs was observed at ~425 nm in 6 min and then steadily increased at 30, 60, 90 and 120 min. The formation of Ag NPs and the reduction of silver ions occurred readily after 60 min. The digital photograph of the coloured reaction of the solution is shown in the inset of Fig 1. The structural morphology, size and crystallinity of the synthesised Ag NPs were further confirmed by TEM, HRTEM, SAED and XRD pattern shown in Fig. 2 (a), (b), (c) and (d), respectively. It is apparent from the TEM images that Ag NPs are predominantly spherical and

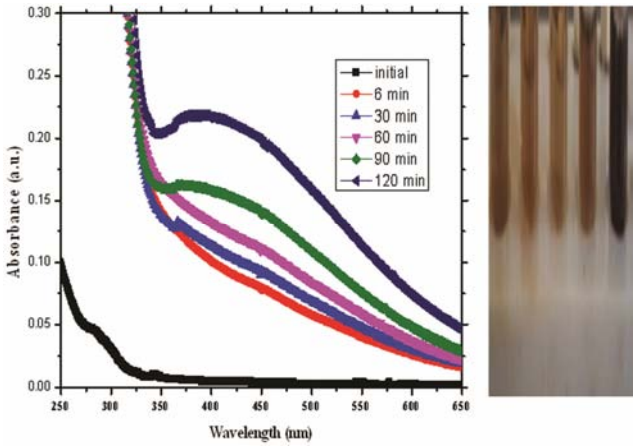

Fig. 1 — UV-visible spectral evolution of the Ag NPs solution recorded as a function of reaction time (min). Inset of the figure shows the digital photograph of the Ag NPs formed at different reaction time in increasing order (from left to right).

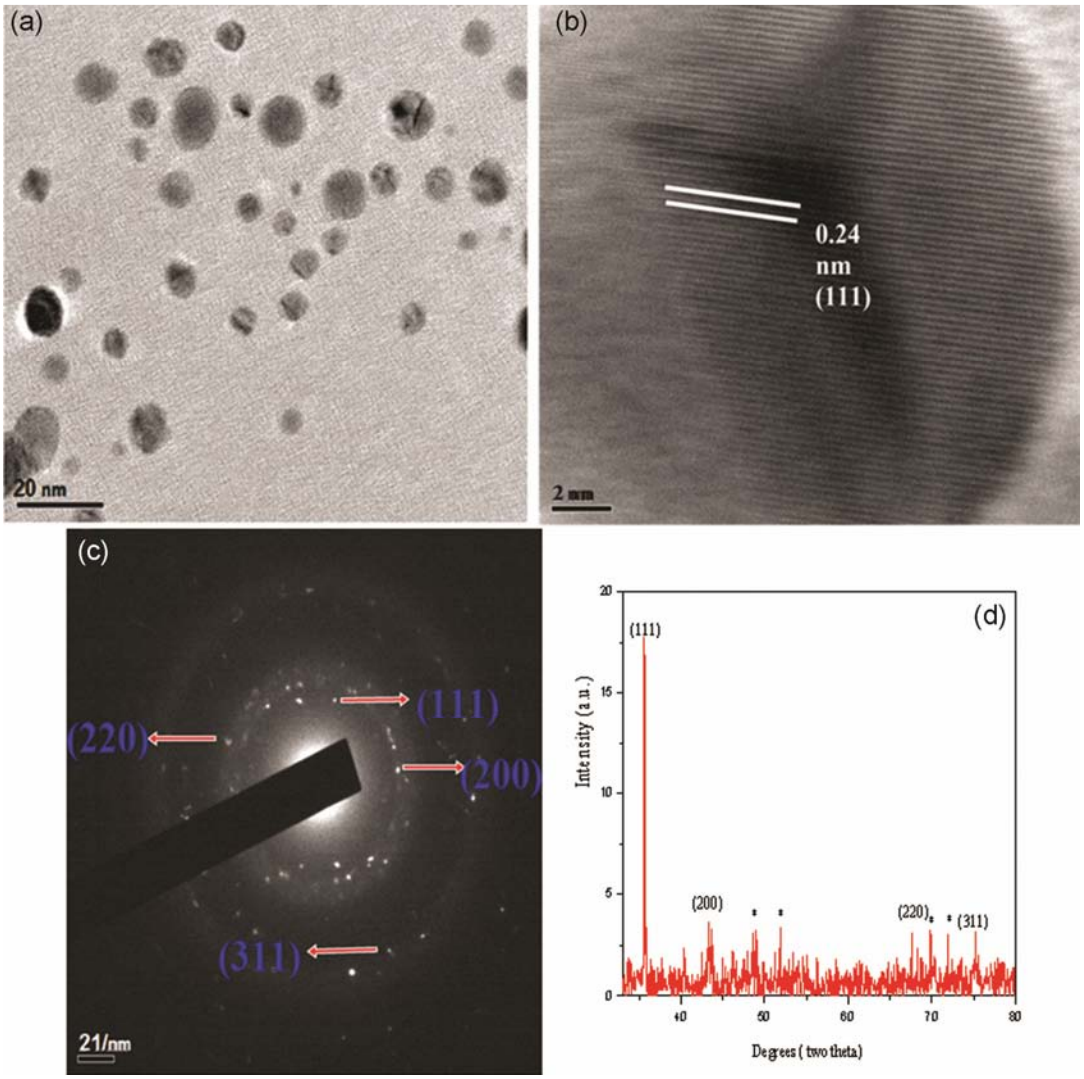

Fig. 2 — (a), (b), (c) and (d) represents the TEM, HRTEM, SAED and XRD image of the Ag NPs respectively.

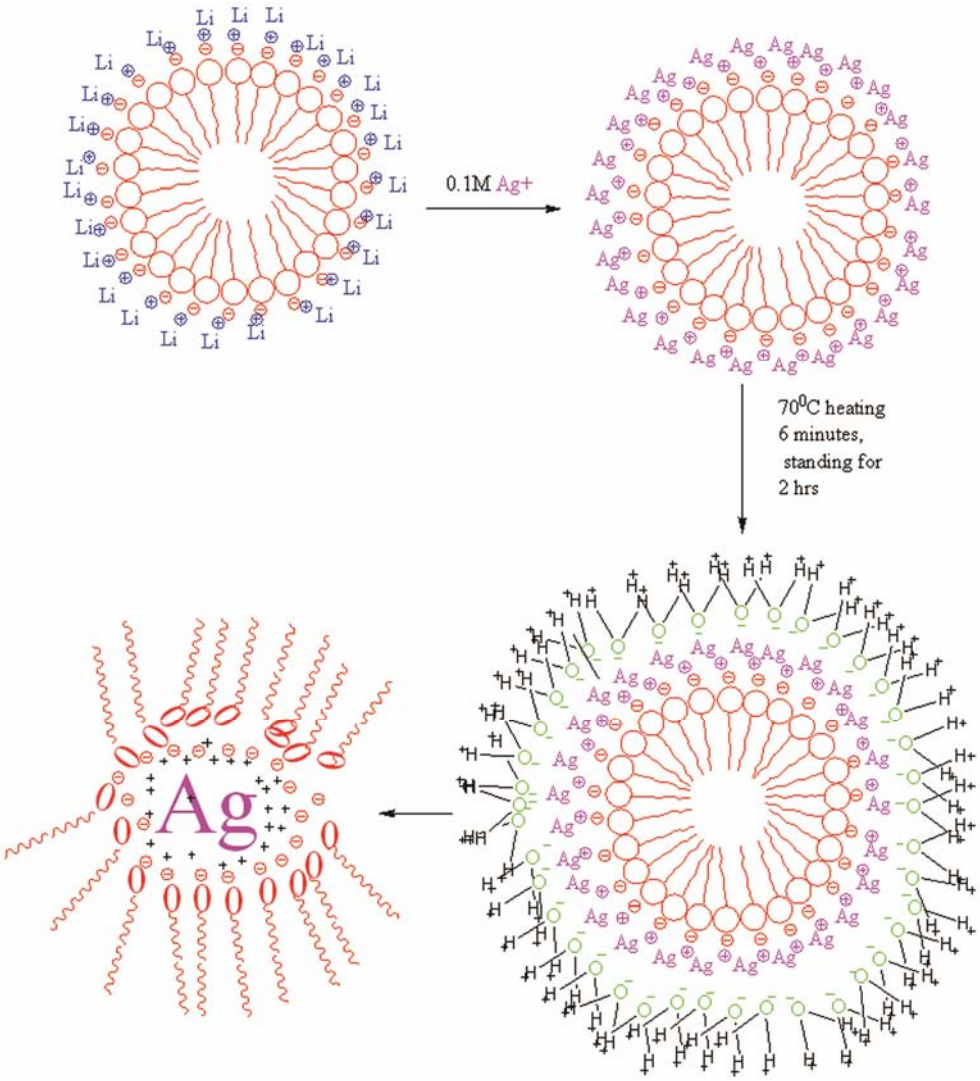

Fig. 3 — Probable mechanism of the Ag NPs.

polydispersed in nature with an average size of the majority NPs in the range of ~7-15 nm. The TEM images revealed that a dark region is surrounded by a faint thin shell (micelles) that stabilizes NPs. The polycrystalline nature of particles can be evidenced from the concentric diffraction ring pattern in a SAED analyses as shown in Fig. 2(c). These could be indexed corresponding to the reflections from the (111), (200), (220) and (311) lattice planes of face centered cubic (fcc) structure of the Ag NPs[12]. The fringe spacing calculated from Fig. 2(b) is found to be about 0.24 nm and corresponds to (111) lattice plane of face centered cubic (fcc) structure of Ag NPs.

Figure 2 (d) depicts the XRD pattern of the prepared Ag NPs. The XRD pattern confirms the face-centered–cubic (fcc) lattice (JCPDS file no. 04-0783) with strong diffraction peaks at 2θ values of 38.5, 44, 66, and 77 degrees, and corresponds to (111), (200), (220) and (311) crystal planes, respectively. The (200), (220) and (311) Bragg reflections are weak and broadened relative to the intense (111) reflection. This feature indicated that the nanocrystals are (111)–oriented as confirmed by the HRTEM images[13]. In addition to the Bragg peaks representation of face centered cubic (fcc) of Ag nanocrystals, additional unassigned peaks are also observed suggesting that the crystallization of other phases occurred on the surface of the nanoparticles[14].

Mechanism

The formation of Ag NPs in the medium can be visualised by the mechanism as shown in Fig. 3. The aqueous LDS solution (60 mM) consists of anionic micelles in which the aliphatic chains are pointed

towards the core, while the head groups are pointed towards polar molecules. The Li^+ ions screen the electrostatic repulsion between the head groups. Due to high reduction potential of Ag^+ ions than Li^+ ions, addition of aqueous $AgNO_3$(0.1M) solution can lead to the displacement of Li^+ ions present on the anionic micelle surface. Hence Ag^+ ions screen the electrostatic repulsion between the head groups. During heating at 70°C, the breaking of non-covalent hydrogen bonds between water molecules is promoted and on subsequent cooling, new bond formation takes place between the Ag^+ ions and water molecules due to electrostatic attraction. This may activate Ag^+ ion at the interface of negatively charged micelle and water molecules to be in dynamic equilibrium. Now Ag^+ ions and dodecylsulphate anions at the interfacial region, do participate in the redox reaction with negatively charged micelle surface acting as a base for both the reduction of Ag^+ ions and growth of nanoparticles.

With increasing growth of Ag NPs clusters, adsorption of positively charged ions gathers at the surface (predominantly Ag^+ ions and H^+ ions). The monomers are being attracted towards the positively charged NPs surface because of the dynamic equilibrium between anionic micelles and its monomers. This protects them by forming an inverse micelle[15]. Due to the increased density of the growing NPs, they diffused at the bottom of the container, while the aqueous soluble oxidised product of dodecyl sulphate anion was removed by decantation. As mentioned above, the dark region covered by a faint thin shell (found in the TEM micrographs) can be explained as the network of dodecyl anion molecules i.e., inverse micelle formed by dodecyl sulphate anion molecules covering the reduced Ag atoms.

Reduction of 4-NP to 4-AP

To investigate the catalytic efficiency of the Ag NPs, the reduction of 4-NP in the presence of $NaBH_4$ as a model reaction was monitored[16]. It is observed that 4-NP in aqueous medium has a maximum absorption at 317 nm. But when freshly prepared $NaBH_4$ solution is added, there was a red shift from 317 nm to 403 nm, and the light yellow colour of the solution changes to intense yellow because of the formation of 4-nitrophenolate ions in alkaline condition. The peak at 403 nm remains unchanged even for a couple of days in the absence of any catalyst.

Addition of 150 µL of 10% Ag NPs solution into the reaction mixture caused a gradual fading of the characteristic yellow colour due to 4-NP. The complete bleaching of the yellow colour of the 4-NP solution was quantitatively monitored spectro-photometrically with time. This is due to the reduction of 4-NP to 4-amino phenol (4-AP). A new peak centred at 420 nm due to the SPR of Ag NPs was observed after completion of the reduction (at 1200 sec). In the mean time, a new peak at 298 nm appeared with progressive increase in intensity (Fig. 4 (a), which is attributed to the typical absorption of 4-AP.These result, suggests that the catalytic reduction of 4-NP exclusively yielded 4-AP without any side products[17]. The complete reduction can be summarized in Scheme 1.

The rate constant (k) for this reaction has been determined from the linear plot of ln (A_t/A_0) versus reduction time, and the constant was estimated to be 6.96×10^{-4} s^{-1}.

Now, the reduction of 4-NP was examined in three different micelles. In micelles, a weak hydrophobic force operates between the 4-nitrophenolate ion and the micelle, and the micelles build wrapper–like barriers surrounding the metal particles, whereas BH_4^- tends to remain outside the dynamic barrier due to lack of hydrophobic part. The reduction rate in SDS is comparable to that in aqueous media as the adsorption of the phenolate ions onto the catalyst doesn't get disturbed as the negatively charged SDS micelle prevented the incorporation of 4-NP. However, in case of CPC (a cationic surfactant), due to the presence of both hydrophobic and hydrophilic interactions between the phenolate ions, adsorption of the substrate was retarded which decreased the rate to a considerable extent. However, in non-ionic surfactant (TX-100), only hydrophilic interactions occurs which give rise to an intermediate reaction rate. These can be represented in Scheme 2.

Hence, the reaction rate followed the sequence: H_2O~SDS >TritonX-100>CPC which has been depicted in Fig. 4 (b).

Photocatalytic degradation of methyl violet 6B dye

Methyl violet 6B dye is a triphenyl methane dye. The degradation of the dye does not take place immediately when irradiated with sunlight. Initially, dye degradation was identified by colour change. In the beginning, the colour of the dye was dark violet which changed into light violet and ultimately colourless after 240 min incubation with Ag NPs while exposed to sunlight.

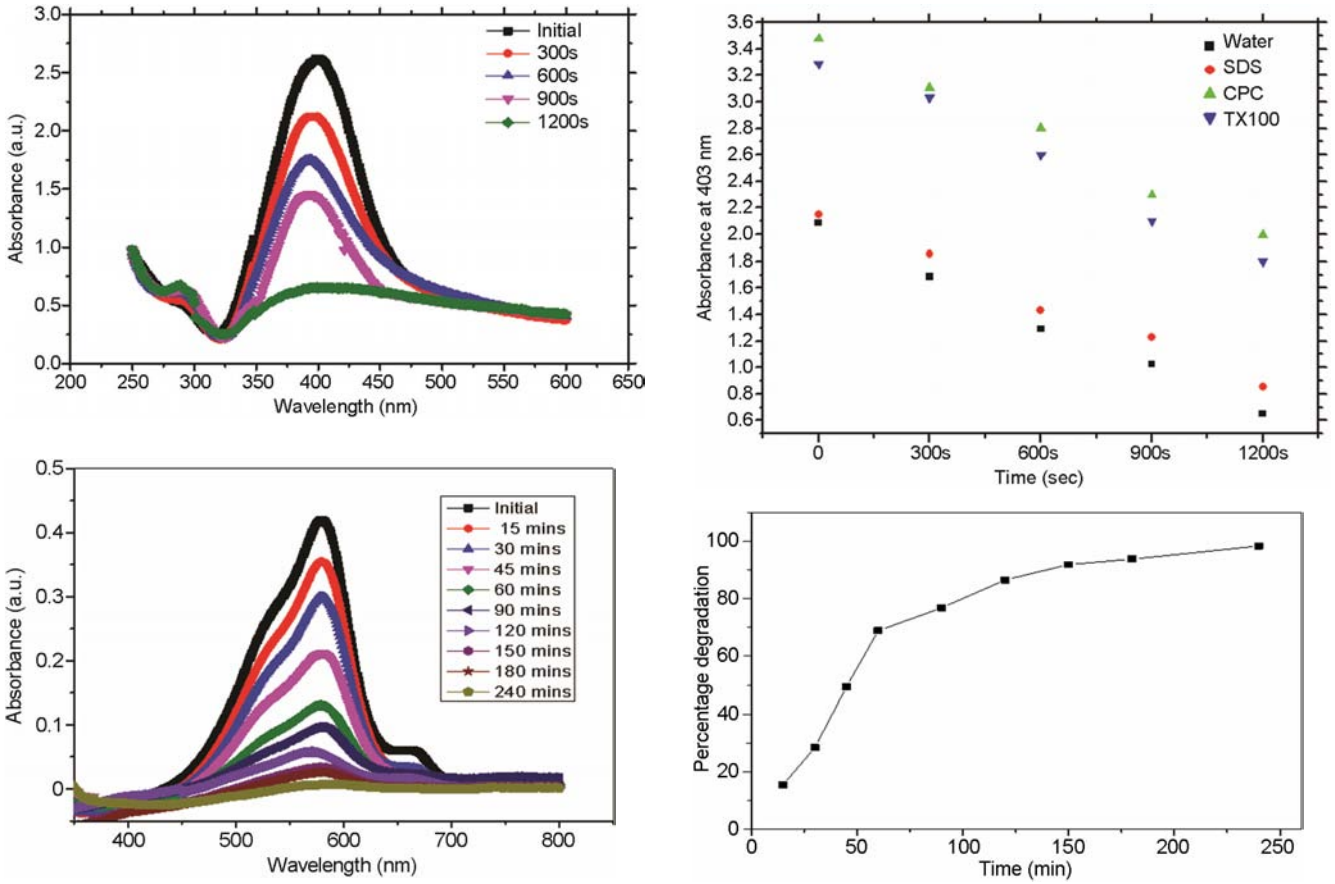

Fig. 4 — (a) UV-vis absorption spectra recorded of 60 µL (6.07×10^{-3} M) 4-NP+ 350 µL (0.1M) $NaBH_4$ + 150 µL 10% Ag NPs in aqueous solution; (b) Absorbance vs time (sec) plot for the reduction of 4-NP prompted by Ag NPs as catalyst; (c) UV-vis absorption spectra for photo degradation of methyl violet dye using Ag NPs; (d) Efficiency (%) with irradiation time for photo degradation of methyl violet dye using Ag NPs and (e) Plot of ln (C_0/C_t) vs irradiation time for photo degradation of methyl violet dye using Ag NPs.

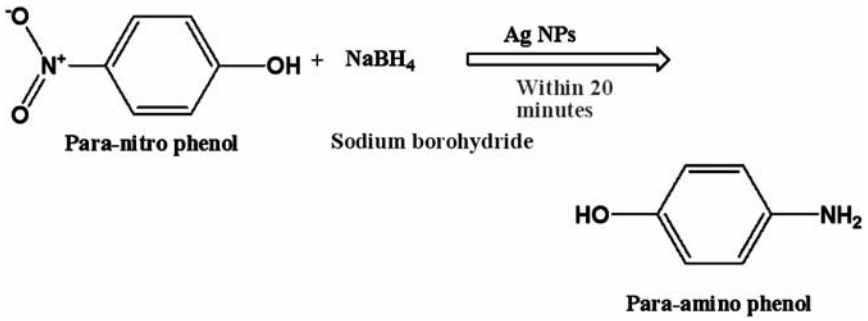

Scheme 1

UV-vis absorption spectra for the degradation of methyl violet 6B using Ag NPs at different time in the visible region is shown in Fig. 4(c). From the plot it is observed that, as the exposure time increases, the concentration of methyl violet 6B dye decreases, which is shown by the decrease in absorption intensity of the UV-vis spectra. It can be seen that the intensity of absorption peak gradually decreases with increase in sunlight irradiation time.

The percentage efficiency of NPs was determined using Equation (2). Figure 4(d) depicts the plot of percentage efficiency with sunlight irradiation time. The plot shows that as the irradiation time increases the efficiency of NPs to degrade methyl violet 6B dye also increases. The percentage of degradation efficiency of Ag NPs was calculated as 98.3% at 240 min. The apparent rate constant for degradation of methyl violet 6B was determined using Equation (3).

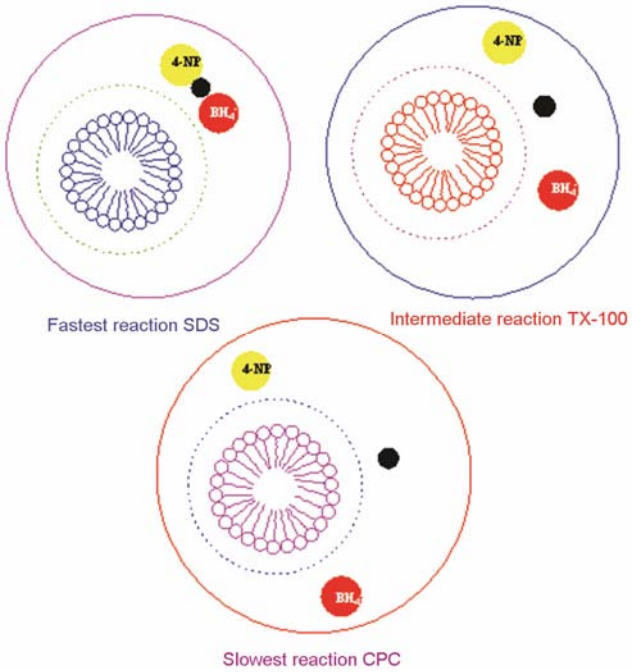

Scheme 2

The plot of ln (C_0/C_t) with irradiation time was plotted, where the slope represents the rate constant for the degradation of the dye (1.72×10^{-2} min^{-1})**.** It was observed that 98.3% of the dye was degraded photochemically within 240 min using Ag NPs by solar irradiation.

The photocatalytic mechanism can be related by two parts namely; photo and catalysis. The first portion is related with light material interaction which comprises of photon absorption charge carrier creation and dynamics, and also surface trapping. The second portion is connected to the surface radical formation and surface reactivity that is interaction between O_2, H_2O, and organic pollutant. Hence, the photocatalytic activity mainly relies on the crystalline quality, and specific surface area is found to be the most fruitful structural parameter[18]. As a whole, the photocatalytic activities of Ag NPs in the visible light may be explained due to the excitation of SPR, which is actually the oscillation of charge density that can propagate at the interface between the dielectric medium and the metal.

Conclusion

A one pot, simple, fast, cost effective, non-toxic and environment friendly method for the synthesis of Ag NPs depicting the dual functional properties of LDS has been described. The catalytic role of the Ag NPs in the reduction of 4-NP in aqueous as well in micellar media and also the photodegradation of the methyl violet 6B dye under solar irradiation has been established.

Acknowledgement

The authors acknowledge TEQIP-II of NIT Silchar for providing the financial assistance, SAIF–NEHU Shillong and Gauhati University for providing the TEM and XRD facilities, respectively.

References

1 Burda C, Chen X, Narayanan R & El-Sayed MA, *Chem Rev*, 105 (2005) 1025.
2 McFarland A D & Van Deeyne R P, *Nano Lett*, 3 (2003) 1057.
3 El-Sayed M A, *Acc Chem Res*, 34 (2001) 257.
4 Henglein, *Chem Mater*, 10 (1998) 444.
5 Okumura M, Tsubota S, Iwamoto M & Haruta M, *Chem Lett*, 4 (1998) 315.
6 Xie J P, Lee J Y, Wang D I C & Ting Y P, *Small,* 3 (2007) 672.
7 Perreux L & Loupy A, *Tertrahedron*, 57 (2001) 9199.
8 Kumazawa H, Inoue M & Kasuya T, *Ind Eng Chem Res*, 42 (2003) 3237.
9 Mendez D H & Mosquera M I M, *J Agric Food Chem*, 49 (2001) 3584.
10 Yu J G, Yu H G, Chen B, Zhao X J, Yu J C & Ho W K, *J Phys Chem B*, 107 (2003) 13871.
11 Ghasemi S, Rahimnejad S, Setayesh S R, Rohani S & Gholami M R, *J Hazard Mater*, 172 (2009) 1573.
12 Guzman M G, Dille J & Godet S, *World Acad Sci Eng & Technol*, 67 (2008) 357.
13 Ankamwar B, Chaudhary M & Sastry M, *Syn React Inorg Met-Org Nano- Met Chem*, 35 (2005) 19.
14 Philip D, Unni C,Aromal S A & Vidhu V K, *Spectrochim Acta*, Part A 78 (2011) 899.
15 Sinha T, Gude V & Rao N V S, *Adv Sci Eng Med*, 4 (2012) 1.
16 Murugadoss A & Chattopadhyay A, *J Phys Chem C*, 112 (2008) 11265.
17 An Q, Yu M, Zhang Y, Ma W, Guo J & Wang C, *J Phys Chem*, C,116 (2012) 22432.
18 Kavitha S R, Umadevi M , Janani S R , Balkrishnan T & Ramanibai R, *Spectrochim Acta Part A,* 127 (2014) 115.